Proceedings of the Sixteenth International Conference on
Computational Structures Technology
Edited by: P. Iványi, J. Kruis and B.H.V. Topping
Civil-Comp Conferences, Volume 14, Paper 3.3
Civil-Comp Press, Edinburgh, United Kingdom, 2026
ISSN: 2753-3239, doi: 10.4203/ccc.14.3.3

Cost Optimisation of Steel Structures Exposed to Fire

T. Světlík and M. Čermák

Department of Mathematics, VSB - Technical University of Ostrava, Czechia

Abstract

This paper presents a size optimisation approach for steel structures exposed to fire and designed according to EN 1993-1-2. The main focus is on unprotected steel members, for which the incremental computation of the steel temperature is replaced by an explicit continuous surrogate model. The surrogate is constructed from Eurocode-based heat-transfer calculations and fitted using an L_∞ regression formulation. For a prescribed fire-resistance time, it maps the cross-section parameters directly to the steel temperature, thereby avoiding repeated incremental temperature calculations during optimisation while preserving differentiability of the fire-design constraints.

The approach is implemented in MATLAB and applied to an elevated steel connecting corridor with a thirty-minute fire-resistance requirement. Three design variants are considered: an ambient-temperature design, an unprotected fire design, and a protected fire design that includes the cost of passive fire protection. The resulting costs are compared and used to discuss the influence of fire-design requirements and passive protection on the optimal design.

Keywords: steel structure, frame structure, structural fire design, size optimisation, cost optimisation, temperature surrogate

1 Introduction

Fire resistance is one of the governing requirements in the design of steel structures. Although steel is a non-combustible material, its mechanical properties deteriorate significantly at elevated temperature. Consequently, a member that satisfies the usual ultimate limit state requirements at normal temperature may lose a substantial part of its load-bearing capacity during fire exposure. The structural fire design of steel members therefore requires the evaluation of the thermal action, the resulting steel temperature, the corresponding reduction of material properties, and the resistance of the member at the prescribed fire-resistance time [2–4, 8].

In practical design, the required fire resistance can be achieved by different strategies. One possibility is to increase the steel cross-sections so that the structure retains sufficient load-bearing capacity even after the temperature-dependent reduction of yield strength and stiffness. Another possibility is to apply passive fire protection, which reduces the heating of the steel members and allows the steel structure to remain closer to the ambient-temperature design. These two strategies lead to different structural weights and different cost contributions. Therefore, the choice between an unprotected and a protected design should not be based only on structural feasibility, but also on the resulting economic efficiency.

Structural optimisation provides a suitable framework for comparing such design alternatives, because it allows the required constraints and cost contributions to be considered simultaneously. Size optimisation of steel structures has been widely studied, both in the context of mathematical programming and metaheuristic optimisation methods [5, 12]. In most standard formulations, the objective function is related to the steel mass or cost, while the constraints represent strength, stability, serviceability, and practical geometric requirements. When fire resistance is included, the optimisation problem becomes more involved because the member resistance depends not only on the cross-section geometry, but also on the temperature reached during the required fire-exposure time.

For unprotected steel members, the temperature development depends on the section factor, the shadow effect, and the prescribed fire-exposure time. If the steel temperature is evaluated by incremental heat-transfer analysis during every optimisation step, the computational cost increases and the relation between the design variables and the fire-design resistance remains implicit. This is inconvenient for repeated structural optimisation, where the fire-design constraints have to be evaluated many times for changing cross-sectional dimensions.

The aim of this paper is to formulate a size optimisation approach for steel structures exposed to fire in which the temperature of unprotected members is represented by a continuous surrogate model. The steel temperature is first computed numerically according to the Eurocode heat-transfer formulation for a range of effective section parameters. For selected fire-resistance times, the resulting discrete temperature data are then approximated by rational polynomial functions. The regression parameters are determined by an L_∞-type formulation, which minimises the maximum absolute approximation error over the computed temperature data. This is suitable for the present application because the surrogate model is used inside design constraints, where local approximation errors should be controlled rather than only minimised in an average sense. The adopted rational approximation is related to classical minimax approximation concepts [7, 11, 16].

The fitted temperature surrogate is introduced into the structural optimisation problem through the effective section parameter. For unprotected members, the surrogate temperature determines the temperature-dependent reduction factors of yield strength and Young's modulus, which are subsequently used in the fire-design constraints. For protected members, a simplified formulation is adopted in which the required fire resistance is assumed to be provided by a prescribed passive protection system. In this case, the steel members are checked using ambient-temperature resistance constraints, while the cost of passive fire protection is included in the objective function through the protected surface area.

The proposed formulation is demonstrated on an elevated steel connecting corridor with a prescribed R30 fire-resistance requirement. Three design variants are compared: an ambient-temperature ultimate limit state design, an unprotected R30 fire design, and a protected R30 fire design. The benchmark is used to quantify the influence of the fire-resistance requirement on the steel mass and total cost, and to compare the economic efficiency of increasing the steel cross-sections with the use of passive fire protection.

2 Fire design of steel structures according to Eurocode

The fire design of steel structures according to Eurocode is treated as an accidental design situation [1–3]. The general form of the structural verification remains similar to the design at normal temperature, but the mechanical properties of steel are modified according to the temperature reached during fire exposure. Therefore, the resistance and stiffness of a steel member exposed to fire are not evaluated using the material properties at $20\,^{\circ}\mathrm{C}$, but using temperature-dependent values.

For a prescribed fire-exposure time t_R, the steel temperature has to be determined first. The corresponding temperature-dependent material properties are then used in the structural resistance checks. In the present work, this relation is used to connect the cross-section geometry, the fire-induced temperature increase, and the resulting structural resistance within the size optimisation problem.

2.1 Reduced material properties at elevated temperature

For structural steel at elevated temperature, Eurocode introduces reduction factors for the effective yield strength and for the slope of the linear elastic range [3]. These factors are defined as

$$k_{y,\theta} = \frac{f_{y,\theta}}{f_y}, \qquad k_{E,\theta} = \frac{E_{a,\theta}}{E_a}, \tag{1}$$

where f_y and E_a denote the yield strength and Young's modulus at normal temperature, while $f_{y,\theta}$ and $E_{a,\theta}$ denote the corresponding values at the steel temperature θ_a. The reduction factors given by Eurocode are shown in Figure 1.

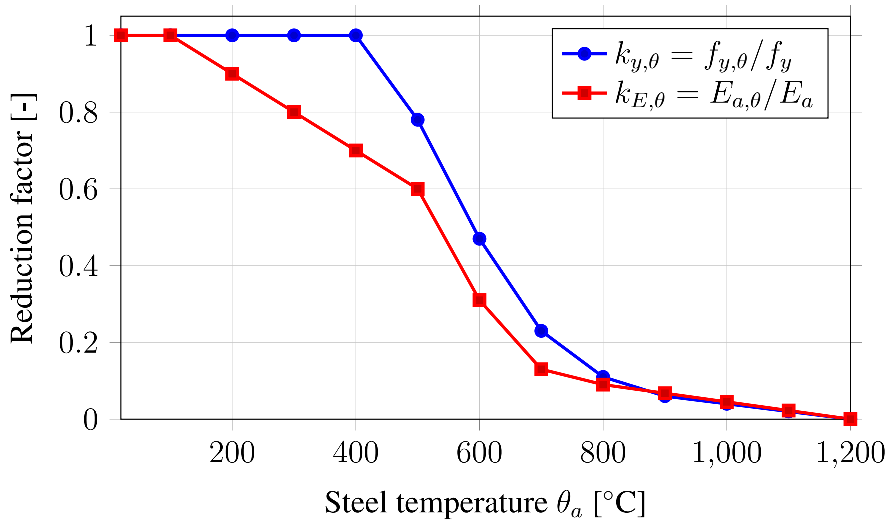

Figure 1: Reduction factors for structural steel at elevated temperature.

The yield-strength reduction factor $k_{y,\theta}$ directly affects the cross-section resistance according to the elevated-temperature design rules of EN 1993-1-2 [3]. For example, for a member loaded in compression, the axial cross-section resistance at elevated temperature can be expressed as

$$N_{\mathrm{c,fi},\theta,\mathrm{Rd}} = k_{y,\theta} \frac{\gamma_{M,0}}{\gamma_{M,\mathrm{fi}}} N_{\mathrm{c,Rd}}, \tag{2}$$

where $N_{\mathrm{c,Rd}}$ is the design cross-section compression resistance at normal temperature.

The effect of elevated temperature is also reflected in member stability. For flexural buckling, the relative slenderness in fire can be written as

$$\bar{\lambda}_\theta = \frac{L_{\mathrm{cr}}}{i\lambda_{1,\theta}}, \qquad \lambda_{1,\theta} = \pi \sqrt{\frac{k_{E,\theta} E_a}{k_{y,\theta} f_y}}, \tag{3}$$

where L_{cr} is the buckling length and i is the radius of gyration. The buckling resistance in fire is then obtained as

$$N_{\mathrm{b,fi},\theta,\mathrm{Rd}} = \chi_{\mathrm{fi}} \left(\bar{\lambda}_\theta\right) N_{\mathrm{c,fi},\theta,\mathrm{Rd}}, \tag{4}$$

where $\chi_{\mathrm{fi}}(\bar{\lambda}_\theta)$ is the buckling reduction factor expressed as a function of the relative slenderness in fire. Thus, temperature influences the member resistance in two ways. The factor $k_{y,\theta}$ reduces the cross-section resistance directly, while both $k_{y,\theta}$ and $k_{E,\theta}$ affect the buckling resistance through $\bar{\lambda}_\theta$.

2.2 Temperature development of unprotected steel members

Since the reduction factors $k_{y,\theta}$ and $k_{E,\theta}$ depend on the steel temperature θ_a, the temperature development of the member has to be evaluated before the fire-design resistance checks are performed. The fire exposure is described by the gas temperature θ_g. In this work, the nominal standard temperature–time curve according to EN 1991-1-2 is used [2]. The gas temperature is given by

$$\theta_g(t) = 20 + 345 \log_{10} (8t + 1), \tag{5}$$

where t is the time in minutes and θ_g is obtained in °C. In the heat-transfer calculation below, the time increment Δt is taken in seconds.

For an unprotected steel member, the temperature increment $\Delta\theta_a$ during the time interval Δt is computed as

$$\Delta\theta_a = k_{\text{sh}} \frac{A_m}{V} \frac{\dot{h}_{\text{net}} (\theta_g, \theta_a)}{\rho_a c_a(\theta_a)} \Delta t, \tag{6}$$

where A_m/V is the section factor, A_m is the exposed surface area of the member per unit length, V is the volume of the member per unit length, $\rho_a = 7850\,\text{kg/m}^3$ is the density of steel, and $c_a(\theta_a)$ is the temperature-dependent specific heat of steel. The temperature-increment formulation and the heat-transfer components follow the Eurocode approach for unprotected steel members [3, 8].

The coefficient k_{sh} accounts for the shadow effect. If the shadow effect is neglected, $k_{\text{sh}} = 1$, which gives a conservative estimate of the steel temperature. For cross-section types for which the Eurocode shadow-effect correction is applicable, the correction factor may be expressed as [3]

$$k_{\text{sh}} = \frac{[A_m/V]_b}{A_m/V}, \tag{7}$$

where $[A_m/V]_b$ is the box value of the section factor.

The net heat flux $\dot{h}_{\text{net}}$ is the heat flux transferred from the fire gases to the steel surface. It is expressed as the sum of the convective and radiative parts,

$$\dot{h}_{\text{net}} (\theta_g, \theta_a) = \dot{h}_{\text{net,c}} (\theta_g, \theta_a) + \dot{h}_{\text{net,r}} (\theta_g, \theta_a), \tag{8}$$

where

$$\dot{h}_{\text{net,c}} (\theta_g, \theta_a) = \alpha_c (\theta_g - \theta_a) \tag{9}$$

and

$$\dot{h}_{\text{net,r}} (\theta_g, \theta_a) = \phi \varepsilon_f \varepsilon_m \sigma \left[(\theta_g + 273.15)^4 - (\theta_a + 273.15)^4 \right]. \tag{10}$$

Here, $\alpha_c = 25\,\text{W/(m}^2\text{K)}$ is the coefficient of heat transfer by convection, $\phi = 1.0$ is the configuration factor, $\varepsilon_f = 1.0$ is the emissivity of the fire, $\varepsilon_m = 0.7$ is the surface emissivity of the member, and $\sigma = 5.67 \cdot 10^{-8}\,\text{W/(m}^2\text{K}^4)$ is the Stefan–Boltzmann constant. In this formulation, the effective radiation temperature is taken equal to the gas temperature of the standard fire curve.

The specific heat $c_a(\theta_a)$, which enters the temperature increment in Equation (6), is taken from the Eurocode temperature-dependent data [3]. It is defined as

$$c_a(\theta_a) = \begin{cases} 425 + 0.773\theta_a - 1.69 \cdot 10^{-3}\theta_a^2 + 2.22 \cdot 10^{-6}\theta_a^3, & 20 \leq \theta_a < 600, \\ 666 + \dfrac{13002}{738 - \theta_a}, & 600 \leq \theta_a < 735, \\ 545 + \dfrac{17820}{\theta_a - 731}, & 735 \leq \theta_a < 900, \\ 650, & 900 \leq \theta_a \leq 1200. \end{cases} \tag{11}$$

Here, θ_a is inserted in $^\circ\mathrm{C}$ and $c_a(\theta_a)$ is obtained in $\mathrm{J}/(\mathrm{kg\,K})$. The corresponding curve is shown in Figure 2.

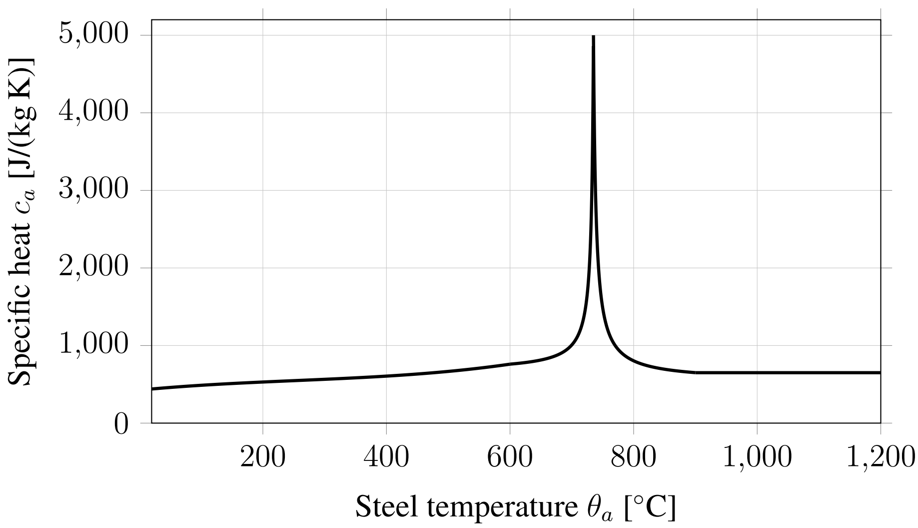

Figure 2: Specific heat of steel as a function of temperature.

The temperature values $\theta_a(t)$ are obtained by applying Equation (6) successively in time, starting from the initial steel temperature $\theta_a(0) = 20\,^\circ\mathrm{C}$. At each time step, the gas temperature θ_g is obtained from Equation (5), while the current steel temperature θ_a enters both the heat flux $\dot{h}_{\mathrm{net}}(\theta_g, \theta_a)$ and the specific heat $c_a(\theta_a)$.

A useful consequence of Equation (6) is that the influence of the cross-section on the temperature calculation enters through the product $k_{\mathrm{sh}} A_m/V$. Therefore, the shadow effect, the cross-section shape, and the cross-section dimensions can be represented by a single effective section parameter

$$\xi = k_{\mathrm{sh}} \frac{A_m}{V}. \tag{12}$$

Within the adopted temperature model, this makes it possible to use one temperature approximation for different steel cross-sections represented by the same value of ξ.

2.3 Protected steel members

The temperature development described in the previous subsection corresponds to an unprotected steel member. If passive fire protection is applied, the heat transfer to the steel is reduced by the insulating layer. In contrast to the unprotected case, the temperature development of a protected member depends not only on the steel cross-section, but also on the thermal conductivity, density, specific heat, thickness, and arrangement of the protection material [3, 4, 8].

In this conference contribution, the detailed heat-transfer analysis of protected members is not included in the optimisation model. The type and thickness of the passive fire protection system are assumed to be selected outside the optimisation procedure so that the prescribed fire-resistance class is satisfied. The optimisation therefore does not determine the protection thickness or the residual temperature increase of the protected steel member explicitly.

This assumption should not be interpreted as stating that the protected steel remains at ambient temperature during fire exposure. Rather, it represents a simplified design strategy in which the required fire resistance is assigned to an externally specified passive protection system. The structural optimisation then accounts for the economic influence of this design strategy through a surface-related protection cost. This simplification is adopted in order to compare, within a compact conference-paper formulation, two alternative ways of satisfying the required fire resistance: increasing the steel cross-sections of unprotected members or applying passive fire protection to a lighter ambient-temperature design.

3 Regression approximation of steel temperature

Although the incremental temperature calculation follows directly from the Eurocode formulation, it is not convenient for repeated use in structural optimisation. In each evaluation of the structural design, the temperature of every unprotected member would have to be obtained by time integration. To avoid this repeated computation, the numerically evaluated temperature response is replaced by a continuous regression approximation.

Using Equation (6), the steel temperature was evaluated for a range of effective section parameters ξ and fire exposure times t. The resulting data form a temperature surface

$$\theta_a = \theta_a(t, \xi), \tag{13}$$

as shown in Figure 3.

For practical fire-resistance checks, the complete temperature history is not required. The relevant quantities are the steel temperatures at prescribed fire-exposure times, such as R15, R30, R45, or R60. By fixing the exposure time $t = t_R$, the computed temperature surface $\theta_a(t, \xi)$ is reduced to the one-dimensional relation

$$\theta_{a,R}(\xi) = \theta_a(t_R, \xi). \tag{14}$$

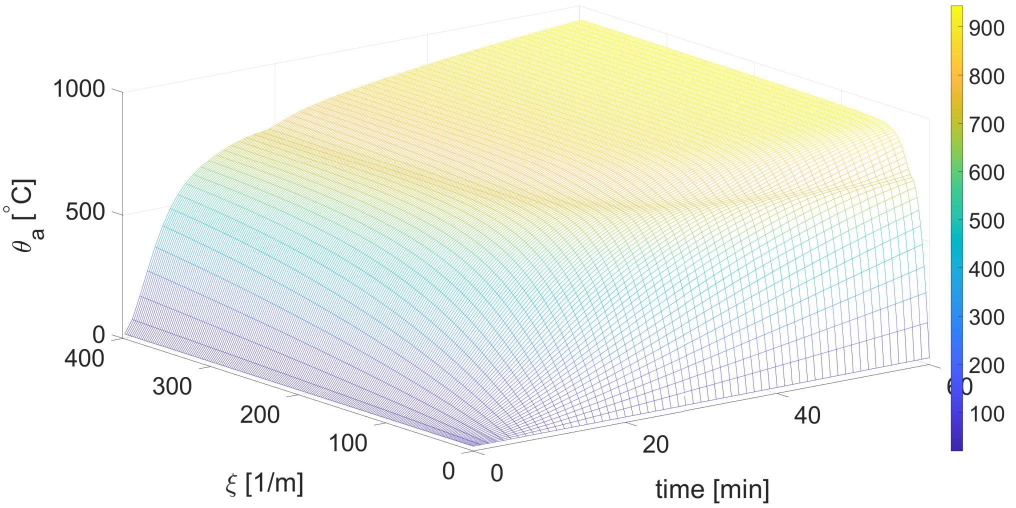

Figure 3: Computed steel temperature as a function of fire exposure time t and effective section parameter $\xi = k_{\text{sh}} A_m / V$.

The corresponding temperature curves are shown in Figure 4.

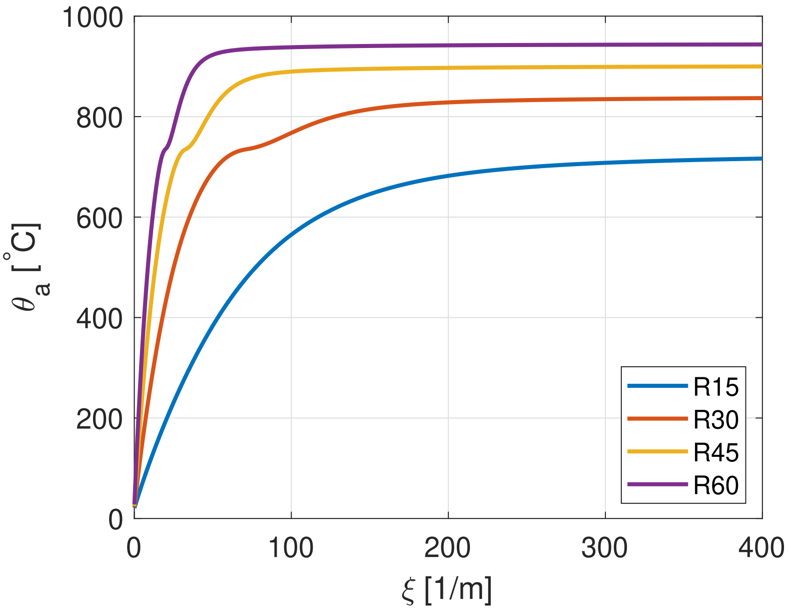

Figure 4: Computed steel temperature for selected fire-exposure times as a function of the effective section parameter $\xi = k_{\text{sh}} A_m / V$.

These curves are used as the basis for the regression approximation introduced next.

3.1 L_∞ regression problem

For a prescribed fire-exposure time t_R, the numerical solution of the heat-transfer problem provides a finite set of computed temperature values

$$\mathcal{D}_R = \{(\xi_i, \theta_{a,R,i})\}_{i=1}^{N_R}, \tag{15}$$

where N_R is the number of computed data points, ξ_i denotes the effective section parameter, and $\theta_{a,R,i}$ is the corresponding steel temperature computed at time $t = t_R$.

Since the temperature values are available only at discrete points, they are approximated by a continuous regression function

$$\widehat{\theta}_{a,R}(\xi; \mathbf{p}), \tag{16}$$

where $\mathbf{p}$ is the vector of regression parameters. In the present work, the approximation is considered in the form of a rational polynomial function

$$\widehat{\theta}_{a,R}(\xi; \mathbf{p}) = \frac{a_0 + a_1\xi + \cdots + a_n\xi^n}{1 + b_1\xi + \cdots + b_m\xi^m}, \tag{17}$$

where n and m denote the polynomial degrees of the numerator and denominator, respectively. The corresponding vector of regression parameters is given by

$$\mathbf{p} = \begin{bmatrix} a_0 & a_1 & \cdots & a_n & b_1 & \cdots & b_m \end{bmatrix}^{\mathrm{T}}. \tag{18}$$

The constant term in the denominator is fixed to one in order to remove the scaling ambiguity of the rational function.

The commonly used least-squares approach minimises the sum of squared residuals and therefore controls the approximation error in an average sense. As a result, larger local errors may be compensated by smaller errors at other data points. In the present case, however, the regression function is used as a surrogate model in the subsequent structural fire-design problem. Therefore, it is not sufficient to obtain a small average error. Instead, the approximation error should remain consistently small over all computed temperature values. For this reason, a discrete L_∞-type formulation is adopted.

The regression parameters are determined by minimising the maximum absolute difference between the computed temperatures and the approximating function. The corresponding regression problem is written as

$$\min_{\mathbf{p}} \left\| \boldsymbol{\theta}_{a,R} - \widehat{\boldsymbol{\theta}}_{a,R}(\mathbf{p}) \right\|_\infty, \tag{19}$$

where

$$\boldsymbol{\theta}_{a,R} = \begin{bmatrix} \theta_{a,R,1} & \theta_{a,R,2} & \cdots & \theta_{a,R,N_R} \end{bmatrix}^{\mathrm{T}} \tag{20}$$

and

$$\widehat{\boldsymbol{\theta}}_{a,R}(\mathbf{p}) = \begin{bmatrix} \widehat{\theta}_{a,R}(\xi_1; \mathbf{p}) & \widehat{\theta}_{a,R}(\xi_2; \mathbf{p}) & \cdots & \widehat{\theta}_{a,R}(\xi_{N_R}; \mathbf{p}) \end{bmatrix}^{\mathrm{T}}. \tag{21}$$

Equivalently, the problem can be expressed in the epigraph form

$$
\begin{aligned}
\min_{\mathbf{p},\varepsilon} \quad & \varepsilon \\
\text{s.t.} \quad & -\varepsilon \leq \theta_{a,R,i} - \widehat{\theta}_{a,R}(\xi_i;\mathbf{p}) \leq \varepsilon, \qquad i = 1,\ldots,N_R, \\
& \varepsilon \geq 0.
\end{aligned}
\tag{22}
$$

Here, ε represents an upper bound on the absolute approximation error over all computed temperature values in $\mathcal{D}_R$. Since the optimisation is performed with respect to both the regression parameters $\mathbf{p}$ and the error bound ε, the solution provides the parameter vector corresponding to the smallest attainable value of ε for the selected rational form.

The fitted relation $\widehat{\theta}_{a,R}(\xi;\mathbf{p})$ is used in the following section as a continuous temperature model for the fire-resistance assessment within the size-optimisation problem.

4 Size optimisation problem under fire exposure

Size optimisation aims to determine the cross-sectional dimensions of the structural members such that a prescribed objective function is minimised while the required design constraints are satisfied. In the present work, the structural topology and the finite element mesh are assumed to be fixed. The optimisation variables are therefore only the geometric parameters of the cross-sections assigned to the individual members.

Let the structure be composed of a finite set of members $\mathcal{E} = \{1, 2, \ldots, n_e\}$, where each index $e \in \mathcal{E}$ denotes one structural member represented by a beam element in the finite element model. Each member e has a fixed length l_e and is assigned a vector of cross-sectional design variables $\mathbf{x}_e$. The complete vector of design variables is written as

$$
\mathbf{x} = \begin{bmatrix} \mathbf{x}_1^{\mathrm{T}} & \mathbf{x}_2^{\mathrm{T}} & \cdots & \mathbf{x}_{n_e}^{\mathrm{T}} \end{bmatrix}^{\mathrm{T}} \in \mathbf{\Omega} \subset \mathbb{R}^{n_x}, \tag{23}
$$

where n_x is the total number of cross-sectional design parameters. Depending on the adopted cross-section type, $\mathbf{x}_e$ may contain, for example, the height, width, web thickness, or flange thickness of the section.

The admissible design space is described by the polytope

$$
\mathbf{\Omega} = \{\mathbf{x} \in \mathbb{R}^{n_x} : \mathbf{B}\mathbf{x} \leq \mathbf{d}\}, \tag{24}
$$

where the inequality $\mathbf{B}\mathbf{x} \leq \mathbf{d}$ collects the geometric and practical bounds imposed on the cross-sectional parameters. These include positivity requirements on dimensions and mutual relations between parameters, such as enforcing a positive web height, a positive flange thickness, or a prescribed relation between the width and thickness of a cross-section.

In conventional steel design, the objective function is often related to the mass or volume of the structure, and the constraints represent the ultimate limit state requirements at ambient temperature. In the present work, this formulation is extended to structures exposed to fire by introducing temperature-dependent material properties and, in the protected case, the additional cost of passive fire protection.

Two optimisation problems are considered. The first problem corresponds to an unprotected steel structure, where the fire-design constraints are evaluated using temperature-reduced material properties. The second problem corresponds to a protected steel structure, where passive fire protection is assumed to provide the required fire resistance. In this case, the steel members are checked using the ambient-temperature material properties, while the objective function includes both the steel cost and the protection cost.

4.1 Unprotected steel structure

The regression model introduced in the previous section provides a continuous approximation of the steel temperature for a prescribed fire-exposure time t_R. For an unprotected steel member $e \in \mathcal{E}$, the temperature development depends on the effective section parameter

$$\xi_e(\mathbf{x}_e) = k_{\mathrm{sh},e}(\mathbf{x}_e)\frac{A_{m,e}(\mathbf{x}_e)}{V_e(\mathbf{x}_e)}, \tag{25}$$

where $A_{m,e}(\mathbf{x}_e)$ is the exposed surface area per unit length, $V_e(\mathbf{x}_e)$ is the steel volume per unit length, and $k_{\mathrm{sh},e}(\mathbf{x}_e)$ is the correction factor for the shadow effect.

The steel temperature of an unprotected member at the prescribed fire-exposure time is then approximated by

$$\theta_{a,R,e}(\mathbf{x}_e) = \widehat{\theta}_{a,R}\left(\xi_e(\mathbf{x}_e); \mathbf{p}_R\right), \tag{26}$$

where $\mathbf{p}_R$ is the vector of regression parameters obtained for the selected fire-exposure time t_R. The temperature-dependent reduction factors can therefore also be expressed as functions of the member design variables,

$$k_{y,R,e}(\mathbf{x}_e) = k_y\left(\theta_{a,R,e}(\mathbf{x}_e)\right), \qquad k_{E,R,e}(\mathbf{x}_e) = k_E\left(\theta_{a,R,e}(\mathbf{x}_e)\right). \tag{27}$$

These member-level quantities are used in the fire design checks, while the corresponding internal forces and displacements are obtained from the global finite element response of the complete structure.

For the unprotected steel structure, the cost is assumed to be proportional to the volume of steel,

$$C_{\mathrm{v}}(\mathbf{x}) = \sum_{e\in\mathcal{E}} c_{\mathrm{v,e}} l_e A_e(\mathbf{x}_e), \tag{28}$$

where $c_{\mathrm{v,e}}$ is the unit cost of steel per unit volume and $A_e(\mathbf{x}_e)$ is the cross-sectional area of steel. The term $l_e A_e(\mathbf{x}_e)$ represents the steel volume of member e.

The corresponding optimisation problem is written as

$$\begin{aligned} \min_{\mathbf{x}} \quad & C_{\mathrm{v}}(\mathbf{x}) \\ \text{s.t.} \quad & c_{\mathrm{ULS}}(\mathbf{x}) \leq \mathbf{0}, \\ & c_{\mathrm{fire},R}(\mathbf{x}) \leq \mathbf{0}, \\ & \mathbf{x} \in \mathbf{\Omega}. \end{aligned} \tag{29}$$

Here, $c_{\mathrm{ULS}}(\mathbf{x})$ denotes the constraints corresponding to the ambient-temperature ultimate limit state, while $c_{\mathrm{fire},R}(\mathbf{x})$ denotes the fire-design constraints for the prescribed fire-exposure time t_R. The fire-design constraints are evaluated using the steel temperature from Equation (26) and the corresponding reduction factors from Equation (27).

4.2 Protected steel structure

For the protected steel structure, the detailed heat-transfer analysis through the protection layer is not included in the optimisation model. The passive fire protection system is assumed to be prescribed in advance and selected so that the required fire-resistance class is satisfied. Consequently, the structural optimisation determines the steel geometry using ambient-temperature resistance constraints, while the cost of passive fire protection is included in the objective function.

In the protected formulation, all members included in the fire-design model are assumed to be provided with passive fire protection. Besides the cost associated with the amount of structural steel, the optimisation problem also includes the cost of the protection applied to the member surfaces. This protection cost is defined as

$$C_{\mathrm{s}}(\mathbf{x}) = \sum_{e \in \mathcal{E}} c_{\mathrm{s},e} l_e A_{m,e}(\mathbf{x}_e). \tag{30}$$

Here, $c_{\mathrm{s},e}$ is the unit cost of passive fire protection per unit surface area and $A_{m,e}(\mathbf{x}_e)$ is the exposed surface area per unit length of member e. The product $l_e A_{m,e}(\mathbf{x}_e)$ therefore represents the surface area to which passive fire protection is applied.

The protected optimisation problem is then written as

$$\begin{aligned} \min_{\mathbf{x}} \quad & C_{\mathrm{v}}(\mathbf{x}) + C_{\mathrm{s}}(\mathbf{x}) \\ \text{s.t.} \quad & c_{\mathrm{ULS}}(\mathbf{x}) \leq \mathbf{0}, \\ & \mathbf{x} \in \mathbf{\Omega}. \end{aligned} \tag{31}$$

The absence of explicit fire-design constraints in Equation (31) does not imply that the protected steel member remains at ambient temperature during fire exposure. Rather, it reflects the modelling assumption that the required fire resistance is ensured by an externally selected passive protection system. Therefore, the protected formulation should be interpreted as a simplified cost-comparison model between two design strategies, not as a detailed thermal design model for the protection layer.

The two optimisation problems allow a direct comparison between two fire-design strategies. In the unprotected case, the required fire resistance must be achieved by increasing the steel cross-sections so that the members retain sufficient resistance after the temperature-dependent reduction of material properties. In the protected case, the steel members may remain closer to the ambient-temperature optimum, but the total cost is increased by the surface-related cost of passive fire protection.

5 Numerical results

5.1 Regression approximation results

The L_∞ regression problem was solved for the selected fire-exposure times R15, R30, R45, and R60. The epigraph formulation in Equation (22) was solved in MATLAB using `fmincon` [15]. The effective section parameter was considered in the interval $\xi \in [0.1, 400]\ \mathrm{m}^{-1}$. Before evaluating the rational approximation, this interval was mapped to the normalised variable

$$s(\xi) = 2\frac{\xi - \xi_{\min}}{\xi_{\max} - \xi_{\min}} - 1, \qquad \xi_{\min} = 0.1\ \mathrm{m}^{-1}, \qquad \xi_{\max} = 400\ \mathrm{m}^{-1}. \tag{32}$$

The fitted surrogate model for the steel temperature at the prescribed fire-exposure time t_R was written as

$$\hat{\theta}_{a,R}(\xi) = \frac{a_{0,R} + a_{1,R}s(\xi) + \cdots + a_{n,R}s^n(\xi)}{1 + b_{1,R}s(\xi) + \cdots + b_{m,R}s^m(\xi)}. \tag{33}$$

The denominator constant term is fixed to one, and the coefficients multiply powers of the normalised variable $s(\xi)$. The fitted coefficient vectors are listed in Appendix A.

The fitted surrogate curves are shown in Figure 5, together with the computed temperature values used in the regression.

The polynomial degrees and the maximum absolute approximation errors are summarised in Table 1. The value $\varepsilon_{\max}$ denotes the maximum absolute difference between the computed steel temperature and the fitted surrogate model over all regression points. For all selected fire-exposure times, the maximum absolute error remains below 1 °C.

Table 1: Polynomial degrees and maximum absolute errors of the fitted temperature surrogate models.

Fire class	n	m	$\varepsilon_{\max}$ [°C]
R15	3	2	0.9871
R30	5	4	0.8718
R45	5	5	0.9424
R60	10	10	0.8993

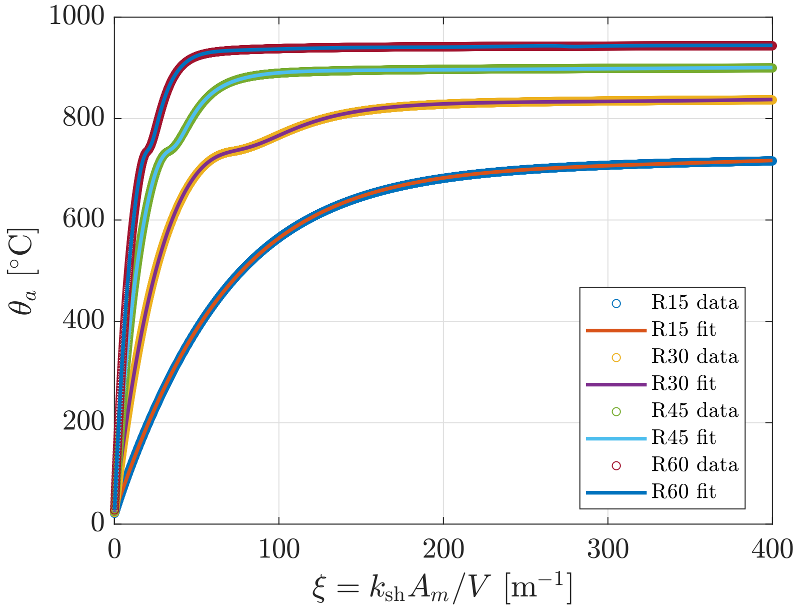

Figure 5: Computed steel temperatures and fitted rational surrogate models for selected fire-exposure times.

For the structural optimisation benchmark presented in the following subsection, the R30 surrogate model was used to evaluate the steel temperature of unprotected members. This allowed the temperature-dependent material reduction factors to be computed directly from the current cross-sectional dimensions, without repeating the incremental heat-transfer analysis during each optimisation step.

5.2 Steel corridor

The proposed optimisation approach was applied to a real steel structure designed as an elevated connecting corridor between two parts of a building. The benchmark represents a practical design situation in which the prescribed fire-resistance class R30 can be satisfied either by increasing the steel cross-sections of an unprotected structure or by applying passive fire protection to a lighter steel design. In addition to these two fire-design variants, the structure was also optimised for the standard ambient-temperature ultimate limit state. This case provides a reference design without any fire-resistance requirement. The original three-dimensional RFEM model of the structure is shown in Figure 6.

The structure consists of two main longitudinal trusses connected by transverse members and supported by steel columns. The loads considered in the benchmark include self-weight, additional permanent loads, snow loads, and wind loads. The three-dimensional RFEM model was used to define the geometry, supports, and load effects of the complete structure.

The ambient-temperature design constraints were evaluated using the standard ultimate-

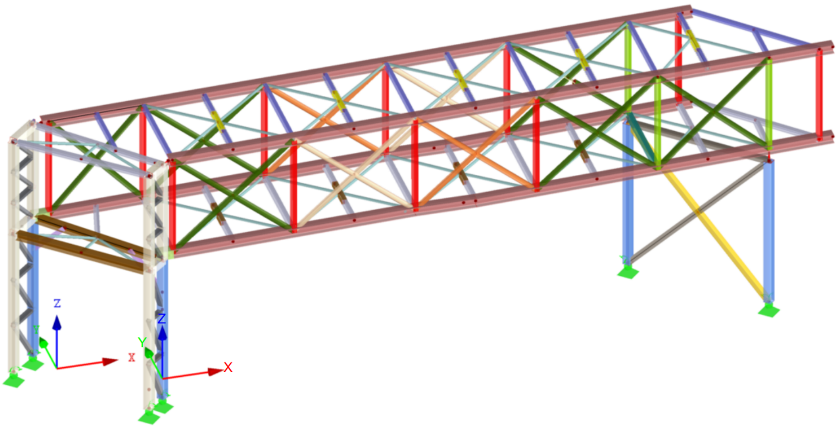

Figure 6: Three-dimensional RFEM model of the elevated steel connecting corridor.

limit-state load combinations. The fire-design constraints for the unprotected R30 variant were evaluated using the accidental fire-design situation according to the Eurocode framework [1–3]. Thus, the reduced material properties at the prescribed fire-exposure time were combined with the corresponding accidental fire load case. The same accidental fire load case was used as the design basis for selecting the passive fire protection in the protected R30 variant.

For the optimisation, one main longitudinal truss was extracted from the full structure and represented by a two-dimensional structural model. The load effects obtained from the three-dimensional model were transferred to this simplified model as equivalent loads. The size optimisation problems were solved in MATLAB using an inexact restoration approach [13, 14]. The resulting cross-sectional dimensions were subsequently exported back to RFEM for verification using the corresponding two-dimensional RFEM model.

The admissible cross-section families were selected according to the original structural documentation. The main truss chords were restricted to HEB sections, the columns to RHS sections, and the diagonal and bracing members to CHS sections. All members were made of steel grade S355. The same structural model, loading, supports, material grade, member grouping, and admissible cross-section families were used for all design variants.

The total structural cost was evaluated from the volume of steel used in the individual members. Since different cross-section families have different market prices, a separate unit volume cost was assigned to each family. The unit costs of the steel cross-section families were obtained from the online catalogue of Ferona, a.s. [6]. The adopted unit volume costs were $15700\ \mathrm{EUR/m^3}$ for HEB sections, $10990\ \mathrm{EUR/m^3}$ for RHS sections, and $18840\ \mathrm{EUR/m^3}$ for CHS sections. These values were used as representative input parameters for the comparative benchmark.

For the protected design, the unit price of the fire-protective coating was adopted from publicly available price lists for fire-protective coatings on steel structures [9, 10]. The adopted unit protection cost was $c_\mathrm{s} = 38.4\ \mathrm{EUR/m^2}$. Since the actual cost of passive fire protection depends on the selected system, required resistance class, protected surface area, and project conditions, this value is used as a representative cost parameter for the comparative benchmark.

The optimisation results are summarised in Table 2. The ambient-temperature ULS design resulted in a steel mass of $1.087\ \mathrm{t}$ and a total cost of $2183\ \mathrm{EUR}$. This design is used as the reference case for the relative cost comparison. The unprotected R30 design required substantially larger steel cross-sections, increasing the steel mass to $3.249\ \mathrm{t}$ and the total cost to $6529\ \mathrm{EUR}$, which corresponds to 2.991 times the cost of the ambient-temperature design. In contrast, the protected R30 design retained the same steel mass as the ambient-temperature design, $1.087\ \mathrm{t}$, while the total cost increased to $3635\ \mathrm{EUR}$ due to the additional cost of passive fire protection. This corresponds to 1.665 times the cost of the ambient-temperature design.

Table 2: Optimisation results for the elevated connecting corridor.

Design variant	Steel mass [t]	Total cost [EUR]	Relative cost [-]
Ambient-temperature ULS design	1.087	2183	1.000
Unprotected R30 design	3.249	6529	2.991
Protected R30 design	1.087	3635	1.665

The optimised unprotected and protected designs are shown in Figure 7 and Figure 8, respectively. The unprotected design requires larger steel cross-sections because the members have to retain sufficient resistance after the temperature-dependent reduction of material properties. In the protected design, passive fire protection allows the steel structure to remain close to the ambient-temperature optimum, while the additional protection cost is included directly in the total cost evaluation.

For the investigated structure, the ambient-temperature design provides a useful reference for quantifying the economic influence of the R30 requirement. If the R30 requirement is satisfied without passive fire protection, the required steel mass increases from $1.087\ \mathrm{t}$ to $3.249\ \mathrm{t}$, and the total cost becomes almost three times larger than the ambient-temperature cost. The protected R30 design avoids this increase in steel mass, but its total cost remains higher than the ambient-temperature design because of the added cost of the fire-protective coating. Compared with the unprotected R30 design, the protected design reduces the steel mass by approximately $66.5\ \%$ and the total cost by approximately $44.3\ \%$. For the investigated structure and the adopted cost parameters, passive fire protection therefore provides a more economical way of satisfying the R30 requirement than increasing the steel cross-sections alone.

6 Conclusion

This paper presented a size optimisation formulation for steel structures exposed to fire. For unprotected members, the steel temperature at a prescribed fire-exposure time is expressed using a surrogate model depending on the effective section param-

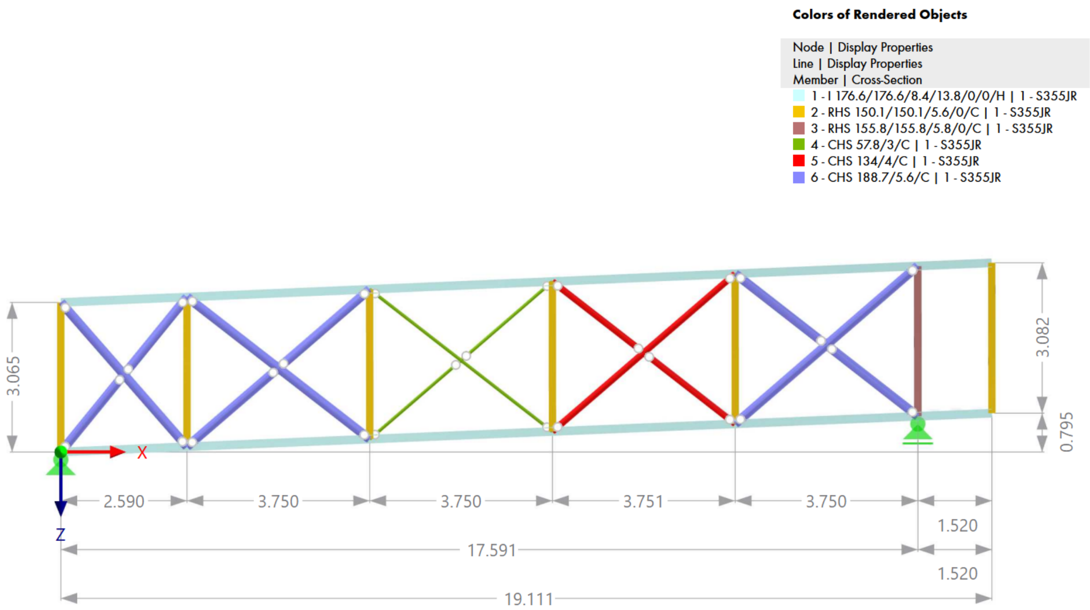

Figure 7: Optimised unprotected design satisfying the R30 fire-resistance requirement without passive fire protection.

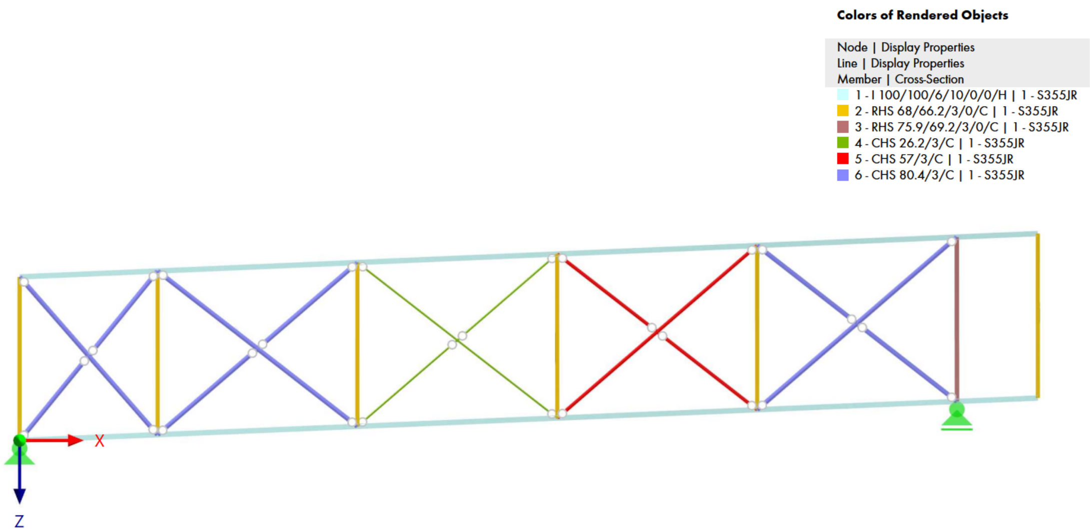

Figure 8: Optimised protected design satisfying the R30 fire-resistance requirement with passive fire protection.

eter $\xi = k_{\mathrm{sh}} A_m / V$. The surrogate was fitted by rational polynomial functions using an L_∞ regression problem, so that the maximum absolute error over the computed temperature data is controlled. For the selected fire-exposure times R15, R30, R45, and R60, the fitted models achieved errors below $1\ ^\circ\mathrm{C}$.

The proposed formulation was applied to an elevated steel connecting corridor with an R30 fire-resistance requirement. The ambient-temperature design resulted in a steel mass of $1.087\ \mathrm{t}$ and a total cost of $2183\ \mathrm{EUR}$. The unprotected R30 design increased the steel mass to $3.249\ \mathrm{t}$ and the cost to $6529\ \mathrm{EUR}$. In contrast, the protected R30 design retained the same steel mass as the ambient-temperature design, while the total cost increased to $3635\ \mathrm{EUR}$ due to the cost of passive fire protection.

For the investigated structure and the adopted cost parameters, passive fire protection led to a lower total cost than increasing the steel cross-sections alone. Compared with the unprotected R30 design, the protected design reduced the steel mass by approximately $66.5\ \%$ and the total cost by approximately $44.3\ \%$. Since the protected-member formulation used in this conference contribution is simplified, future work should include the thickness and thermal properties of the protection system as design variables and evaluate the protected steel temperature explicitly.

Acknowledgements

The work was supported by the Student Grant Competition of VŠB-TUO. The project registration number is SP2026/039.

Declaration of generative AI and AI-assisted technologies in the writing process.

During the preparation of this work, the authors used OpenAI's ChatGPT in order to assist with language refinement and improving the clarity and readability of the text. After using this tool, the authors reviewed and edited the content as needed and takes full responsibility for the content of the publication.

References

[1] EN 1990: Eurocode – Basis of Structural Design, 2002.

[2] EN 1991-1-2: Eurocode 1 – Actions on Structures – Part 1-2: General Actions – Actions on Structures Exposed to Fire, 2002.

[3] EN 1993-1-2: Eurocode 3 – Design of Steel Structures – Part 1-2: General Rules – Structural Fire Design, 2005.

[4] Andrew H. Buchanan and Anthony K. Abu. *Structural Design for Fire Safety*. Wiley, Chichester, 2 edition, 2017.

[5] József Farkas and Károly Jármai. *Optimum Design of Steel Structures*. Springer, Berlin, Heidelberg, 2013.

[6] Ferona, a.s. Ferona online: catalogue of metallurgical material. `https://online.ferona.cz/`, 2026. Accessed: 2 July 2026.

[7] Silviu-Ioan Filip, Yuji Nakatsukasa, Lloyd N. Trefethen, and Bernhard Beckermann. Rational minimax approximation via adaptive barycentric representations. *SIAM Journal on Scientific Computing*, 40(4):A2427–A2455, 2018.

[8] Jean-Marc Franssen and Paulo Vila Real. *Fire Design of Steel Structures*. Ernst & Sohn, Berlin, 2 edition, 2015.

[9] LESTER – Malby a nátěry. Protipožární nátěry Brno – Ceník požárních nátěrů. `https://www.maliripokojubrno.cz/cenik-protipozarni-natery`, 2026. Accessed: 2 July 2026.

[10] LESTER malby – nátěry – tapety. Ceník protipožární nátěry. `https://www.pokoju-maliri.cz/cenik-protipozarni-natery`, 2026. Accessed: 2 July 2026.

[11] Yuji Nakatsukasa and Lloyd N. Trefethen. An algorithm for real and complex rational minimax approximation. *SIAM Journal on Scientific Computing*, 42(5):A3157–A3179, 2020.

[12] M. P. Saka and Z. W. Geem. Mathematical and metaheuristic applications in design optimization of steel frame structures: An extensive review. *Mathematical Problems in Engineering*, 2013:271031, 2013.

[13] Tadeáš Světlík, Martin Mrovec, Lukáš Pospíšil, and Martin Čermák. Size optimisation of 2d frame structures using inexact restoration. In P. Iványi, J. Kruis, and B. H. V. Topping, editors, *Proceedings of the Fifteenth International Conference on Computational Structures Technology*, volume CCC 9 of *Civil-Comp Conferences*, Edinburgh, UK, 2024. Civil-Comp Press. Paper 10.4.

[14] Tadeáš Světlík and Martin Čermák. Size optimization of beam structures with respect to self-weight. In P. Iványi, J. Kruis, and B. H. V. Topping, editors, *Proceedings of the Eighteenth International Conference on Civil, Structural and Environmental Engineering Computing*, volume CCC 10 of *Civil-Comp Conferences*, Edinburgh, UK, 2025. Civil-Comp Press.

[15] The MathWorks, Inc. MATLAB (r2024b), 2024. Numerical computing environment and programming language.

[16] Lloyd N. Trefethen. *Approximation Theory and Approximation Practice*. SIAM, Philadelphia, 2013.

Appendix

A Regression coefficients

The coefficient vectors of the fitted rational temperature surrogate models are listed in this appendix. The surrogate model is evaluated using the normalised effective section parameter $s(\xi)$ defined in Equation (32). The denominator constant term is fixed to one and is therefore not included in the vector $\mathbf{b}_R$. Thus, for each fire-exposure time t_R, the coefficients correspond to the surrogate model defined in Equation (33).

For R15, the coefficient vectors are

$$\mathbf{a}_{15} = \begin{bmatrix} 683.037875990212 \\ 850.069635146370 \\ 214.113462138815 \\ 40.9561208602560 \end{bmatrix}, \qquad \mathbf{b}_{15} = \begin{bmatrix} 1.10707710305676 \\ 0.385336679695949 \end{bmatrix}. \tag{34}$$

For R30, the coefficient vectors are

$$\mathbf{a}_{30} = \begin{bmatrix} 828.982992480415 \\ 3792.01179028991 \\ 6441.12093746648 \\ 4747.02821302958 \\ 1330.92929707772 \\ 61.4049226404794 \end{bmatrix}, \qquad \mathbf{b}_{30} = \begin{bmatrix} 4.54378279845022 \\ 7.71424640605525 \\ 5.71120825164780 \\ 1.56551794525335 \end{bmatrix}. \tag{35}$$

For R45, the coefficient vectors are

$$\mathbf{a}_{45} = \begin{bmatrix} 896.288108753533 \\ 4515.56727946542 \\ 9082.76239971550 \\ 9134.54769665068 \\ 4605.62850462328 \\ 934.554007477582 \end{bmatrix}, \qquad \mathbf{b}_{45} = \begin{bmatrix} 5.03398042473417 \\ 10.1118057622413 \\ 10.1393036327471 \\ 5.07991293892125 \\ 1.01803633076085 \end{bmatrix}. \tag{36}$$

For R60, the coefficient vectors are

$$\mathbf{a}_{60} = \begin{bmatrix} 940.969255050897 \\ 0 \\ 23.0543805677666 \\ 2890.79371609831 \\ -61475.9341552070 \\ -146177.108800298 \\ 111531.780111567 \\ 692224.626590323 \\ 885201.871677289 \\ 491210.512369349 \\ 103927.149860607 \end{bmatrix}, \qquad \mathbf{b}_{60} = \begin{bmatrix} -0.00358886691911414 \\ 0 \\ 3.00147432690863 \\ -65.0636948358443 \\ -154.254558848556 \\ 118.595609138846 \\ 732.246541608693 \\ 936.365628561578 \\ 520.293532966537 \\ 110.388220771997 \end{bmatrix}. \tag{37}$$